Inorg. Chem. **2007**, *46*, 5046–5058

Construction of Ag/1,2,4-Triazole/Polyoxometalates Hybrid Family Varying from Diverse Supramolecular Assemblies to 3-D Rod-Packing Framework

Quan-Guo Zhai, Xiao-Yuan Wu, Shu-Mei Chen, Zhen-Guo Zhao, and Can-Zhong Lu*

State Key Laboratory of Structural Chemistry, Fujian Institute of Research on the Structure of Matter, Chinese Academy of Sciences, Fuzhou, Fujian, 350002, P. R. China

Received March 4, 2007

Eight members of the Ag/1,2,4-triazole/polyoxometalates (POMs) hybrid supramolecular family, namely, $[Ag_4(dmtrz)_4][Mo_8O_{26}]$ (dmtrz = 3,5-dimethyl-1,2,4-triazole, **1**), $[Ag_6(3atrz)_6][PMo_{12}O_{40}]_2 \cdot H_2O$ (3atrz = 3-amino-1,2,4-triazole, **2**), $[Ag_2(3atrz)_2]_2[HPMo^{VI}_{10}Mo^{V}_2O_{40}]$ (**3**), $[Ag_2(dmtrz)_2]_2[HPMo^{VI}_{10}Mo^{V}_2O_{40}]$ (**4**), $[Ag_2(trz)_2]_2[Mo_8O_{26}]$ (trz = 1,2,4-triazole, **5**), $[Ag_2(3atrz)_2][Ag_2(3atrz)_2(Mo_8O_{26})]$ (**6**), $[Ag_4(4atrz)_2Cl][Ag(Mo_8O_{26})]$ (4atrz = 4-amino-1,2,4-triazole, **7**), and $[Ag_5(trz)_4]_2[Ag_2(Mo_8O_{26})] \cdot 4H_2O$ (**8**), were synthesized through hydrothermal reactions of 1,2,4-triazole or its derivatives with appropriate silver salts and molybdates. Crystal structure analysis reveals that the POM-dependent Ag–1,2,4-triazolate units in these hybrid compounds form a novel tetranuclear cluster (**1**), a unique double calix[3]arene-shaped hexamer (**2**), zigzag chains (**5** and **6**), helix chains (**3**, **4**, and **8**), and an interesting looped chain (**7**). A series of hydrogen bonding-based supramolecular assemblies varying among the 0-D + 0-D (**1** and **2**), 0-D + 1-D (**3** and **4**), 1-D + 1-D (**5** and **7**), and 1-D + 2-D (**6**) modes between the organomatic cations and POM anions were observed in these structures. Moreover, the inorganic chain $[Ag(Mo_8O_{26})]_n^{3n-}$ in **7** constructed by the building block $[Mo_8O_{26}]^{4-}$ linked only via single Ag^+ ion is unprecedented. Compound **8** is the first high-dimensional framework constructed from the $[Ag_2(Mo_8O_{26})]_n^{2n-}$ rod-shaped subunits. These hybrid supramolecular compounds present interesting photochemical properties. The spectroscopic experiments show that they not only are potential semiconductor materials but also have interesting photoluminescence phenomena, including O → Mo [LMCT] and intraligand [$\pi - \pi^*$] emissions generated by internal heavy metal effect.

Introduction

During the past few years, the interest in the design, synthesis, characterization, and functions of inorganic−organic hybrid supramolecular compounds has been growing extensively.[1] Such hybrid compounds have potential applications in separation and storage materials, molecular recognition media, nonlinear materials, and heterogeneous catalysts.[2] Most of these compounds are composed of d-block metal ions and organic ligands, which are connected through coordination bonds. Usually, the hydrogen bonding (O−H···O, N−H···O, O−H···N, C−H···O, etc.) and aryl packing ($\pi-\pi$ and C−H···π) interactions are most frequently used to assemble inorganic and organic molecules in solid, liquid, or gas phase of these compounds. These intermolecular interactions play important roles in the stabilization of supramolecular aggregates and have led to various different assembly modes.[3] In the case of ionic supramolecular compounds, counterions would also play an important role in the stabilization of the structures of the compounds through the electrostatic interaction.[4] In general, −1-charged small anions, such as, NO_3^-, BF_4^-, PF_6^-, etc., are used as counteranions for cationic metal components.[5] Moreover, several examples have shown that anions are capable of

* To whom correspondence should be addressed. E-mail: czlu@ms.fjirsm.ac.cn; Fax: +86-591-83714946; Tel.: +86-591-83705794.

(1) (a) Lehn, J. M. *Supramolecular Chemistry*; VCH: Weinheim, Germany, 1995. (b) *Supramolecular Organometallic Chemistry*; Haiduc, I., Edelmann, F. T., Eds.; VCH: Weinheim, Germany, 1999.

(2) (a) Hagrman, P. J.; Hagrman, D.; Zubieta, J. *Angew. Chem., Int. Ed.* **1999**, *38*, 2638. (b) Kitagawa, S.; Kitaura, R.; Noro, S. *Angew. Chem., Int. Ed.* **2004**, *43*, 2334. (c) Eddaoudi, M.; Moler, D. B.; Li, H.; Chen, B.; Reineke, T. M.; O'Keeffe, M.; Carpenter, G. B.; Sweigart, D. A. *Acc. Chem. Res.* **2004**, *37*, 1. (d) Bradshaw, D.; Claridge, J. B.; Cussen, E. J.; Prior, T. J.; Rosseinsky, M. J. *Acc. Chem. Res.* **2005**, *38*, 273.

(3) (a) Desiraju, G. R.; Gavezzotti, A. *J. Chem. Soc., Chem. Commun.* **1989**, 621. (b) Desiraju, G. R.; Gavezzotti, A. *Acta Crystallogr., Sect. B* **1989**, *45*, 473. (c) Aacheroy, C. B.; Seddon, K. R. *Chem. Soc. Rev.* **1993**, *22*, 397. (d) Jeffrey, G. A. *An Introduction to Hydrogen Bonding*; Oxford University Press: Oxford, U.K., 1997.

10.1021/ic700415w CCC: $37.00
Published on Web 05/08/2007

directing the formation of some porous entities through either cation−anion interactions or hydrogen-bonding interactions between an organic host and an anionic guest.[6]

Polyoxometalates (POMs), as one kind of significant metal oxide cluster with nanosizes and abundant topologies, have recently been employed as inorganic counterions for constructing inorganic−organic hybrid supramolecular arrays with various organic ligands or metal−organic coordination fragments.[7] Supramolecular assembles based on polyoxometalates (POMs) have been intensively investigated in many important aspects such as catalysis, electrical conductivity, and biological chemistry.[8] Compared to simple inorganic anions, POMs are bigger, have more diverse topologies, have a higher charge, and are more suitable as guest units in the metal−organic host because they lead to larger pores, channels, and cavities. To date, several unique high-dimensional metal−organic frameworks have been synthesized using POMs as templates.[7a,7c,9] A current development is to explore novel lattice architectures resulting from the association of organometallic units and POM anions. During this process, we adopt the Ag/1,2,4-triazole/polyoxometalate system as our research project for the following reasons. First, although M′/ligands/POMs hybrid solids have been studied extensively, less than twenty examples with M′ = Ag have been described to date.[10] It is well-known that the 4d transition metal silver(I) is favorable and fashionable ion for the construction of coordination clusters or polymers because of its coordination diversity and flexible, as well as its positive coordination tendency with various donor atoms, such as O, S, I, P, etc. On the other hand, the silver coordination compounds not only are good candidates for potential conducting materials but also show interesting photophysical and photochemical properties.[11] Second, anions are well-known to be an important factor that affects the structures of Ag(I)-based polynuclear compounds or polymers. However, little is know about this effect of large POM anions to date.[10i] Third, nearly all the organic components studied in the POM-based hybrid family are those ligands containing 2-, 3-, or 4-substituted pyridines, such as 2,2-bpy, 2,2-phen, 4,4-bpy, and so on. In fact, pyridine is just one of many readily available heterocyclic ring systems, which differ in their electronic and structural properties; however, most of them have been surprisingly ignored when people look for building blocks.[12] One such ligand is 1,2,4-triazole and its derivatives, which unite the coordination of both pyrazole and imidazole and exhibit an extensively documented ability to bridge metal ions to afford polynuclear clusters or polymers with unusual structural diversity.[13] As an ongoing research project dealing with the coordination chemistry of 1,2,4-triazole ligands,[14] we report a series of

Scheme 1. 1,2,4-Triazole and Its Derivatives Used in the Current Work

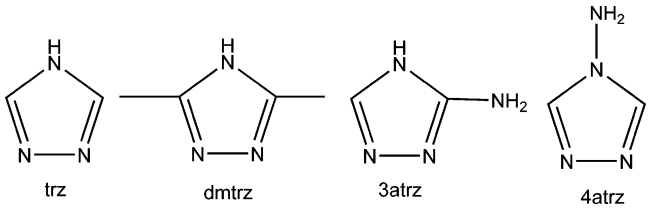

(4) (a) Min, K. S.; Suh, M. P. *J. Am. Chem. Soc.* **2000**, *122*, 6834. (b) Noro, S.; Kitaura, R.; Kondo, M.; Kitagawa, S.; Ishii, T.; Matsuzaka, H.; Yamashita, M. *J. Am. Chem.* Soc. **2002**, *124*, 2568. (c) Du, M.; Guo, Y. M.; Chen, S. T.; Bu, X. H.; Batten, S. R.; Ribas, J.; Kitagawa, S. *Inorg. Chem.* **2004**, *43*, 1287.

(5) (a) Fujita, M.; Yazaki, J.; Ogura, K. *Tetrahedron Lett.* **1991**, *32*, 5589. (b) Leininger, S.; Olenyuk, B.; Stang, P. J. *Chem. Rev.* **2000**, *100*, 853. (c) Fujita, M.; Tominaga, M.; Hori, A.; Therrien, B. *Acc. Chem. Res.* **2005**, *38*, 369 and references therein.

(6) (a) Vilar, R.; Mingos, D. M. P.; White, A. J. P.; Williams, D. J. *Angew. Chem., Int. Ed.* **1998**, *37*, 1258 and references therein. (b) Bianchi, G.; Garcia-España, E.; Bowman-James, K. *Supramolecular Chemistry of Anions*; Wiley-VCH: Weinheim, Germany, 1997.

(7) (a) Inman, C.; Knaust, J. M.; Keller, S. W. *Chem. Commun.* **2002**, 156. (b) Stassen, A. F.; Ferrero, E. M.; Saiz, C. G.; Coronado, E.; Haasnoot, J. G.; Reedijk, J. *Monatsh. Chem.* **2003**, *134*, 255. (c) Yang, L.; Naruke, H.; Yamase, T. *Inorg. Chem. Commun.* **2003**, *6*, 1020. (d) Knaust, J. M.; Inman, C.; Keller, S. W. *Chem. Commun.* **2004**, 492. (e) Ishii, Y.; Takenaka, Y.; Konishi, K. *Angew. Chem., Int. Ed.* **2004**, *43*, 2702. (f) Han, Z. G.; Zhao, Y. L.; Peng, J.; Tian, A. L.; Li, Q.; Ma, J. F.; Wang, E. B.; Hu, N. H. *CrystEngComm* **2005**, *7*, 380. (g) Gamelas, J. A. F.; Santos, F. M.; Felix, V.; Cavaleiro, A. M. V.; Matos Gomes, E.; De Belsley, M.; Drew, M. G. B. *Dalton Trans.* **2006**, 1197.

(8) (a) Special Issue on Polyoxometalates. *Chem. Rev.* **1998**, *98*, 1 and references therein. (b) *Polyoxometalate Chemistry: From Topology Via Self-Assembly to Applications*; Pope, M. T.; Müller, A., Eds.; Kluwer Academic: Dordrecht, The Netherlands, 2001. (c) Hill, C. L.; McCartha, C. M. *Coord. Chem. Rev.* **1995**, *143*, 407. (d) Peloux, C. D.; Dolbecq, A.; Barboux, P.; Laurent, G.; Marrot, J.; Sécheresse, F. *Chem.−Eur. J.* **2004**, *10*, 3026. (e) Coronado, E.; Galán-Mascarós, J. R.; Giménez-Saiz, C.; Gómez-García, C. J.; Martínez-Ferrero E.; Almeida, M.; Lopes, E. B. *Adv. Mater.* **2004**, *16*, 324.

(9) (a) Hagrman, D.; Hagrman, P. J.; Zubieta, J. *Angew. Chem., Int. Ed.* **1999**, *38*, 3165. (b) Zheng, L. M.; Wang, Y. S.; Wang, X. Q.; Korp, J. D.; Jacobson, A. J. *Inorg. Chem.* **2001**, *40*, 1380. (c) Wang, X. L.; Guo, Y. Q.; Li, Y. G.; Wang, E. B.; Hu, C. W.; Hu, N. H. *Inorg. Chem.* **2003**, *42*, 4135. (d) Lisnard, L.; Dolbecq, A.; Mialane, P.; Marrot, J.; Codjovi, E.; Sécheresse, F. *Dalton Trans.* **2005**, 3913−3920. (e) An, H. Y.; Wang, E. B.; Xiao, D. R.; Li, Y. G.; Su, Z. M.; Xu, L. *Angew. Chem., Int. Ed.* **2006**, *45*, 904. (f) Kong, X. J.; Ren, Y. P.; Zheng, P. Q.; Long, Y. X.; Long, L. S.; Huang, R. B.; Zheng, L. S. *Inorg. Chem.* **2006**, *46*, 10702.

(10) (a) Long, D. L.; Xin, X. Q.; Chen, X. M.; Kang, B. S. *Polyhedron* **1997**, *16*, 1259. (b) Villanneau, R.; Proust, A.; Robert, F.; Gouzerth, P. *Chem. Commun.* **1998**, 1491. (c) Rhule, J. T.; Neiwerk, W. A.; Hardcastle, K. I.; Bao, T. D.; Hill, C. L. *J. Am. Chem. Soc.* **2001**, *123*, 12101. (d) Johnson, B. J. S.; Schroden, R. C.; Zhu, C.; Yong, V. G.; Stein, A. *Inorg. Chem.* **2002**, *41*, 2213. (e) Luan, G. Y.; Li, Y. G.; Wang, S. T.; Wang, E. B.; Han, Z. B.; Hu, C. W.; Hu, N. H.; Jia, H. Q. *Dalton Trans.* **2003**, 233. (f) Chen, S. M.; Lu, C. Z.; Yu, Y. Q.; Zhang, Q. Z.; He, X. *Inorg. Chem. Commun.* **2004**, *7*, 1041. (g) Burkholder, E.; Zubieta, J. *Solid State Sci.* **2004**, *6*, 1421. (h) Han, Z. G.; Zhao, Y. L.; Peng, J.; Ma, H. Y.; Liu, Q.; Wang, E. B.; Hu, N. H.; Jia, H. Q. *Eur. J. Inorg. Chem.* **2005**, 264. (i) Ren, Y. P.; Kong, X. J.; Long, L. S.; Huang, R. B.; Zheng L. S. *Cryst. Growth Des.* **2006**, *6*, 572. (j) Abbas, H.; Pickering, A. L.; Long, D. L.; Kögerler, P.; Cronin, L. *Chem.−Eur. J.* **2005**, *11*, 1071. (k) An, H. Y.; Li, Y. G.; Wang, E. B.; Xiao, D. R.; Sun, C. Y.; Xu, L. *Inorg. Chem.* **2005**, *44*, 6062. (l) Shi, Z. Y.; Gu, X. J.; Peng, J.; Yu, X.; Wang, E. B. *Eur. J. Inorg. Chem.* **2006**, 385.

(11) (a) Zheng, S. L.; Zhang, J. P.; Wong, W. T.; Chen, X. M. *J. Am. Chem. Soc.* **2003**, *125*, 6882. (b) Tong, M. L.; Chen, X. M.; Ye, B. H.; Ji, L. N. *Angew. Chem., Int. Ed.***1999**, *38*, 2237.

(12) Steel, P. J. *Acc. Chem. Res.* **2005**, *38*, 243.

(13) (a) Haasnoot, J. G. *Coord. Chem. Rev.* **2000**, *200−202*, 131. (b) Klingele, M. H.; Brooker, S. *Coord. Chem. Rev.* **2003**, *241*, 119. (c) Beckman, U.; Brooker, S. *Coord. Chem. Rev.* **2003**, *245*, 17. (d) Zhang, J. P.; Chen, X. M. *Chem. Commun.* **2006**, 1689 and references therein. (e) Ouellette, W.; Prosvirin, A. V.; Chieffo, V.; Dunbar, K. R.; Hudson, B.; Zubieta, J. *Inorg. Chem.* **2006**, *45*, 9346.

(14) (a) Zhai, Q. G.; Lu, C. Z.; Chen, S. M.; Xu, X. J.; Yang, W. B. *Cryst. Growth Des.* **2006**, *6*, 1393. (b) Zhai, Q. G.; Wu, X. Y.; Chen, S. M.; Lu, C. Z.; Yang, W. B. *Cryst. Growth Des.* **2006**, *6*, 2126. (c) Zhai, Q. G.; Lu, C. Z.; Zhang, Q. Z.; Wu, X. Y.; Xu, X. J.; Chen, S. M.; Chen, L. J. *Inorg. Chim. Acta* **2006**, *359*, 3875. (d) Zhai, Q. G.; Lu, C. Z.; Chen, S. M.; Xu, X. J.; Yang, W. B. *Inorg. Chem. Commun.* **2006**, *9*, 819.

Ag/1,2,4-triazole/POM hybrid solids, namely, $[Ag_4(dmtrz)_4][Mo_8O_{26}]$ (dmtrz = 3,5-dimethyl-1,2,4-triazole, **1**), $[Ag_6(3atrz)_6][PMo_{12}O_{40}]_2 \cdot H_2O$ (3atrz = 3-amino-1,2,4-triazole, **2**), $[Ag_2(3atrz)_2]_2[HPMo^{VI}_{10}Mo^{V}_{2}O_{40}]$ (**3**), $[Ag_2(dmtrz)_2]_2[HPMo^{VI}_{10}Mo^{V}_{2}O_{40}]$ (**4**), $[Ag_2(trz)_2]_2[Mo_8O_{26}]$ (trz = 1,2,4-triazole, **5**), $[Ag_2(3atrz)_2][Ag_2(3atrz)_2(Mo_8O_{26})]$ (**6**), $[Ag_4(4atrz)_2Cl][Ag(Mo_8O_{26})]$ (4atrz = 4-amino-1,2,4-triazole, **7**), and $[Ag_5(trz)_4]_2[Ag_2(Mo_8O_{26})] \cdot 4H_2O$ (**8**). The POM-dependent metal−organic units in these compounds are a novel tetranuclear cluster (**1**), an unprecedented double calyx[3]arene-shaped hexamer (**2**), zigzag chains (**5** and **6**), helix chains (**3**, **4**, and **8**), and a looped chain (**7**). A series of interesting hydrogen bonding-based supramolecular assemblies between the organomatic units and POMs were observed in these structures. Their structure relationship reveals that the POM-templated synthetic approach is suitable for not only high-dimensional metal−organic polymers (2-D or 3-D) but also chain structures or polynuclear clusters. Here, we discuss the supramolecular assemblies and novel photochemical properties of this Ag/1,2,4-triazole/ polyoxometalates hybrid family in detail.

Experimental Section

Materials and Methods. The ligands dmtrz and 4atrz were prepared according to the literature methods.[15] Other reagents and solvents employed were commercially available and were used without further purification. C, H, N, and Mo elemental analyses were determined on an Elementar Vario EL III elemental analyzer. The FT-IR spectra (KBr pellets) were recorded on a PECO (U.S.A.) SpectrumOne spectrophotometer. UV−vis absorption and diffuse reflectance spectra were obtained with a Lamdba900 UV−vis−NIR spectrophotometer at room temperature. Initially, the 100% line flatness of the spectrophotometer was set using barium sulfate ($BaSO_4$). A powder crystal sample of the compound was mounted on the sample holder. The thickness of the sample was approximately 2.00 nm, which was much larger than the individual crystal particles. The fluorescence spectra were measured on powder crystal samples at room temperature using a Cary Eclipse fluorescence spectrophotometer. The excitation slit and emission slit both were 2.5 nm. The X-band ESR spectra were recorded on a Bruker 2000-D-SRC spectrometer on powder crystal materials at 298 K. Thermal stability studies were carried out on a NETSCHZ STA-449C thermoanalyzer under air (40−700 °C range) at a heating rate of 10 °C min^{-1}.

Syntheses. A. $[Ag_4(dmtrz)_4][Mo_8O_{26}]$ (1). A mixture of MoO_3 (0.072 g, 0.50 mmol), $Ag(CH_3CO_2)$ (0.085 g, 0.50 mmol), $Na_2MoO_4 \cdot 2H_2O$ (0.12 g, 0.50 mmol), dmtrz (0.048 g, 0.5 mmol), and H_2O (10 mL) was heated at 180 °C for 5 days under autogenous pressure after adjustment of the pH to ∼4.3 by the addition of 20% tetramethylammonium hydroxide (pH 2.0 after hydrothermal reaction). Colorless block crystals were manually isolated from unidentified powder after the reaction solution cooled gradually (5 °C h^{-1}), washed with water, and air dried. Yield: 0.16 g (∼64% based on Ag). Anal. Calcd (%) for $C_{16}H_{28}Ag_4Mo_8N_{12}O_{26}$: C, 9.59; H, 1.41; N, 8.39; Mo, 38.31. Found (%): C, 9.42; H, 1.50; N, 8.41; Mo, 38.76. IR (solid KBr pellet, cm^{-1}): ν 3458 (br), 3302 (m), 2963 (w), 2832 (w), 1631 (w), 1581 (m), 1556 (w), 1411 (w), 1393 (w), 1376 (w), 1067 (w), 939 (s), 905 (s), 836 (s), 723 (s), 687 (w), 657 (s), 548 (w), 520 (w), 472 (w), 445 (w), 407 (w).

B. $[Ag_6(3atrz)_6][PMo_{12}O_{40}]_2 \cdot H_2O$ (2). A mixture of $H_3[PMo_{12}O_{40}] \cdot xH_2O$ (reference molecular weight = 1825) (0.45 g, 0.25 mmol), Ag_2SO_4 (0.12 g, 0.38 mmol), 3atrz (0.063 g, 0.75 mmol), and H_2O (10 mL) was heated at 180 °C for 5 days under autogenous pressure after adjustment of the pH to ∼2.1 by the addition of dilute H_2SO_4 solution. Pure orange polyhedron crystals were isolated after the reaction solution was cooled gradually (5 °C h^{-1}) to room temperature, washed with water, and air-dried. Yield: 0.54 g (∼90% based on Ag). Anal. Calcd (%) for $C_{12}H_{26}Ag_6Mo_{24}N_{24}O_{81}P_2$: C, 2.99; H, 0.54; N, 6.98; Mo, 47.83. Found (%): C, 3.01; H, 0.55; N, 6.93; Mo, 47.90. IR (solid KBr pellet, cm^{-1}): ν 3340 (br), 1624 (s), 1579 (w), 1547 (w), 1375 (w), 1246 (w), 1060 (s), 981 (w), 969 (w), 950 (s), 869 (m), 845 (w), 791 (s), 593 (w).

C. $[Ag_2(3atrz)_2]_2[HPMo^{VI}_{10}Mo^{V}_{2}O_{40}]$ (3) and $[Ag_2(3atrz)_2][Ag_2(3atrz)_2(Mo_8O_{26})]$ (6). A mixture of $H_3[PMo_{12}O_{40}] \cdot xH_2O$ (0.45 g, 0.25 mmol), $Ag(CH_3CO_2)$ (0.17 g, 1.0 mmol), 3atrz (0.084 g, 1.0 mmol), and H_2O (10 mL) was heated at 180 °C for 5 days under autogenous pressure (initial pH value was ∼2.2 without adjustment). Black polyhedron crystals of **3** and colorless prism crystals of **6** were isolated manually from a yellow unidentified powder after the reaction solution was cooled gradually (5 °C h^{-1}) to room temperature, washed with water, and air-dried. Compound **3**. Yield: 0.22 g (∼34% based on Ag). Anal. Calcd (%) for $C_8H_{12}Ag_4Mo_{12}N_{16}O_{40}P$: C, 3.72; H, 0.47; N, 8.67; Mo, 44.52. Found (%): C, 3.69; H, 0.50; N, 8.63; Mo, 44.63. IR (solid KBr pellet, cm^{-1}): ν 3442 (br), 3412 (m), 3347 (br), 3144 (w), 2919 (w), 2851 (w), 1639 (s), 1572 (w), 1549 (w), 1445 (w), 1300 (w), 1244 (w), 1228 (w), 1166 (w), 1077 (w), 1054 (s), 949 (s), 846 (m), 794 (s), 732 (w), 643 (w), 504 (w). Compound **6**. Yield: 0.05 g (∼10% based on Ag). Anal. Calcd (%) for $C_8H_{16}Ag_4Mo_8N_{16}O_{26}$: C, 4.92; H, 0.83; N, 11.49; Mo, 39.33. Found (%): C, 5.13; H, 0.76; N, 11.68; Mo, 39.21. IR (solid KBr pellet, cm^{-1}): ν 3420 (s), 3334 (w), 3140 (w), 2769 (w), 1643 (s), 1549 (w), 1385 (w), 1295 (w), 1225 (w), 1167 (w), 1058 (m), 997 (w), 939 (s), 895 (m), 839 (w), 747 (w), 684 (w), 630 (w), 523 (w).

D. $[Ag_2(dmtrz)_2]_2[HPMo^{VI}_{10}Mo^{V}_{2}O_{40}]$ (4). A mixture of $H_3[PMo_{12}O_{40}] \cdot xH_2O$ (0.45 g, 0.25 mmol), $Ag(CH_3CO_2)$ (0.17 g, 1.0 mmol), dmtrz (0.097 g, 1.0 mmol), and H_2O (10 mL) was heated at 180 °C for 5 days under autogenous pressure (initial pH value was ∼2.1 without adjustment), followed by slow cooling (5 °C h^{-1}) to room temperature. Almost phase-pure black polyhedron crystals were collected, washed with water, and air-dried. Yield: 0.56 g (∼85% based on Ag). Anal. Calcd (%) for $C_{16}H_{28}Ag_4Mo_{12}N_{12}O_{40}P$: C, 7.27; H, 1.07; N, 6.36; Mo, 43.57. Found (%): C, 7.29; H, 1.12; N, 6.33; Mo, 43.53. IR (solid KBr pellet, cm^{-1}): ν 3447 (m), 3232 (m), 3108 (w), 2816 (w), 1634 (w), 1583 (w), 1561 (w), 1544 (w), 1408 (m), 1373 (m), 1289 (w), 1138 (w), 1060 (s), 962(s), 933 (w), 788 9s), 593 (w), 504 (w).

E. $[Ag_2(trz)_2]_2[Mo_8O_{26}]$ (5). A mixture of $(NH_4)_6Mo_7O_{24} \cdot 4H_2O$ (0.31 g, 0.25 mmol), Ag_2SO_4 (0.31 g, 1.0 mmol), trz (0.069 g, 1.0 mmol), and H_2O (10 mL) was heated at 180 °C for 5 days under autogenous pressure after adjustment of the pH to ∼4.5 by the addition of a dilute H_2SO_4 solution. Pure green block crystals were isolated after the reaction solution was cooled gradually (5 °C h^{-1}) to room temperature, washed with water, and air dried. Yield: 0.36 g (∼75% based on Ag). Anal. Calcd (%) for $C_8H_{12}Ag_4Mo_8N_{12}O_{26}$: C, 5.08; H, 0.64; N, 8.89; Mo, 40.58. Found (%): C, 4.96; H, 0.72; N, 8.90; Mo, 40.12. IR (solid KBr pellet, cm^{-1}): ν 3435 (br), 3115 (w), 2923 (w), 1635 (s), 1496 (w), 1381 (w), 1287 (w), 1263 (w), 1171 (m), 1081 (m), 949 (s), 917 (w), 899 (m), 871 (m), 812 (s), 683 (s), 640 (m), 603 (s), 547 (w), 515 (w), 475 (w).

(15) (a) Herbst, R. M.; Garrison, J. A. *J. Org. Chem.* **1953**, *18*, 872. (b) Baitalik, S.; Dutta, B.; Nag, K. *Polyhedron* **2004**, *23*, 913.

F. $[Ag_4(4atrz)_2Cl][Ag(Mo_8O_{26})]$ (7). A mixture of MoO_3 (0.14 g, 1.0 mmol), $Ag(CH_3CO_2)$ (0.25 g, 1.5 mmol), $Na_2MoO_4 \cdot 2H_2O$ (0.24 g, 1.0 mmol), 4atrz (0.042 g, 0.50 mmol), and H_2O (10 mL) was heated at 180 °C for 5 days under autogenous pressure after adjustment of the pH to ~4.3 by the addition of a dilute HCl solution (pH 1.6 after hydrothermal reaction). Gray block crystals were manually isolated from unidentified powder after the reaction solution cooled gradually, washed with water, and air dried. Yield: 0.39 g (~68% based on Ag). Anal. Calcd (%) for $C_4H_8Ag_5Mo_8N_8O_{26}Cl$: C, 2.49; H, 0.42; N, 5.82; Mo, 39.84. Found (%): C, 2.46; H, 0.56; N, 5.79; Mo, 40.02. IR (solid KBr pellet, cm^{-1}): ν 3434 (br), 3222 (w), 3097 (w), 2976 (w), 1635 (m), 1593 (m), 1130 (w), 1072 (w), 944 (w), 920 (w), 903 (w), 886 (s), 830 (m), 711 (m), 667 (w), 616 (w), 575 (w).

G. $[Ag_5(trz)_4]_2[Ag_2(Mo_8O_{26})] \cdot 4H_2O$ (8). A mixture of $(NH_4)_6Mo_7O_{24} \cdot 4H_2O$ (0.15 g, 0.12 mmol), $Ag(CH_3CO_2)$ (0.25 g, 1.5 mmol), trz (0.069 g, 1.0 mmol), and H_2O (10 mL) was heated at 180 °C for 5 days under autogenous pressure after adjustment of the pH to ~4.3 by the addition of a dilute CH_3COOH solution. Pure red block crystals were isolated after the reaction solution was cooled gradually (5 °C h^{-1}) to room temperature, washed with water, and air dried. Yield: 0.34 g (~88% based on Ag). Anal. Calcd (%) for $C_{16}H_{16}Ag_{12}Mo_8N_{24}O_{30}$: C, 6.22; H, 0.52; N, 10.89; Mo, 24.87. Found (%): C, 6.18; H, 0.64; N, 11.05; Mo, 24.64. IR (solid KBr pellet, cm^{-1}): ν 3435 (br), 2977 (w), 1635 (s), 1501 (w), 1384 (w), 1279 (w), 1148 (w), 1067 (w), 879 (br), 550 (w).

X-ray Crystallography. Suitable single crystals of **1**−**8** were carefully selected under an optical microscope and glued to thin glass fibers. Crystallographic data for all compounds were collected with a Siemens Smart CCD Diffractometer with graphite-monochromated Mo Kα radiation (λ = 0.71073 Å) at T = 293(2) K. Absorption corrections were made using the SADABS program.[16] The structures were solved using the direct method and refined by full-matrix least-squares methods on F^2 by using the SHELX-97 program package.[17] All non-hydrogen atoms were refined anistropically. The positions of the hydrogen atoms attached to carbon and nitrogen atoms were fixed at their ideal positions, and those attached to water oxygen atoms were not located. Crystal data, as well as details of data collection and refinement, for **1**−**8** are summarized in Table 1. The structural characteristics are listed in Table 2.

Results and Discussion

Syntheses. The compounds of this study were prepared in good yields by exploitation of the hydrothermal reactions of 1,2,4-triazole ligands, suitable silver salts, and molybdates at 180 °C for 5 days. The conditions reported in the Experimental Section have been optimized for yields of crystalline products. Two key factors affect the formation of the resulting products: one is the pH value, and the other is the Ag source. It has been well-known that the formation of different polyoxometalate clusters is mainly controlled by the pH values. In our experiments, the pH values were kept at 2.0−2.5 for compounds **2**, **3**, and **4** and at 4.3−4.5 for compounds **1**, **5**, **7**, and **8** or else no products could be obtained or the yield was very low. Compound **6** is a byproduct of **3**, and the search for a suitable synthesis method was unsuccessful. The selection of a suitable Ag source is the second key factor in our syntheses of these compounds. Many failed experiments show that free Ag^+ ions are readily reduced to simple substance Ag or oxidized to black Ag_2O under hydrothermal conditions. Thus, the water-soluble salt $AgNO_3$ is not an ideal Ag source, and therefore, insoluble salts $Ag(CH_3CO_2)$ or Ag_2SO_4 were selected in our experiments. We speculated that the slow release of Ag^+ ions under hydrothermal conditions can provide the chance for their assembly with organic ligands and decrease the probability of oxidation or reduction. The experimental results prove that our selection is right. The successful isolation of these compounds under hydrothermal conditions using $Ag(CH_3CO_2)$ or Ag_2SO_4 as the silver source provides a feasible synthetic route to Ag-based coordination polymers or hybrid materials. Moreover, the Keggin anions in compounds **3** and **4** were reduced under hydrothermal conditions. Since these two compounds both are synthesized in acidic media, we speculated the reduced Keggin anions could be $[HPMo^{VI}_{10}Mo^{V}_2O_{40}]^{4-}$. This result was in agreement with the charge neutrality, crystal color, and ESR spectra.

Description of Crystal Structures. Compound **1** consists of tetranuclear silver coordinated cations $[Ag_4(dmtrz)_4]^{4+}$ and polyoxoanions $[Mo_8O_{26}]^{4-}$, and it crystallizes in the space group $C2/c$ with four formula units in the unit cell. Three crystallographically independent Ag(I) are of linear coordination environments (Ag−N bonds and corresponding N−Ag−N angles = 2.195(4) Å and 140.7(2)° for Ag(1); 2.186(4) Å and 138.4(2)° for Ag(2); 2.130(4), 2.135(4) Å, and 167.0(18)° for Ag(3)). Four Ag(I) atoms were linked by dmtrz ligands through N1,N2-bridging mode to form the coordinated $[Ag_4(dmtrz)_4]^{4+}$ cation (Figure 1). In such a fashion, the Ag···Ag distances vary from 3.246(11) to 3.406(3) Å. A series of such structures with Cu^I as metal center have been reported in our previous report,[14c] and tetranuclear Ag(I) clusters based on triazole ligands are rarely presented to date.[18] It is noted that although the aromatic rings are basically parallel, the distances between the planes of two rings are in the range of 3.754(7)−4.328(8) Å, indicating no significant $\pi-\pi$ stacking interactions. The centrosymmetric $[Mo_8O_{26}]^{4-}$ anion built up from eight edge-shared $\{MoO_6\}$ octahedra is a typical β-octamolybdate.[19] The neutral $[\{Ag(dmtrz)\}_4Mo_8O_{26}]$ was further extended into three−dimensional supramolecular arrays (Figure S1) through weak (N−H···O) and (C−H···O) hydrogen bonds (Table 3). As shown in Figure S1, the overall packing of **1** can be derived from the NaCl structure type. The octamolybdates are coordinated by six $[Ag_4(dmtrz)_4]^{4+}$ clusters in the form of a distorted octahedra with center-to-center distances of 7.394(13), 8.091(12), and 8.960(1) Å. The silver clusters are connected by six octamolybdates anions octahedrally as well. Two similar NaCl-type supramolecular intercluster compounds had been reported to date: one is constructed

(16) Sheldrick, G. M. *SADABS, Program for Area Detector Adsorption Correction*; Institute for Inorganic Chemistry, University of Göttingen: Göttingen, Germany, 1996.
(17) Sheldrick, G. M. *SHELXL-97, Program for Solution of Crystal Structures;* University of Göttingen: Göttingen, Germany, 1997.
(18) Wang, Y.; Yi, L.; Yang, X.; Ding, B.; Cheng, P.; Liao, D. Z.; Yan, S. P. *Inorg. Chem.* **2006**, *45*, 5822.
(19) Klemperper, W. G.; Shum, W. *J. Am. Chem. Soc.* **1976**, *98*, 8291.

Table 1. Crystal Data and Structure Refinements for Compounds **1**−**8**

	1	**2**	**3**	**4**
empirical formula	$C_{16}H_{28}Ag_4Mo_8N_{12}O_{26}$	$C_{12}H_{26}Ag_6Mo_{24}N_{24}O_{81}P_2$	$C_8H_{13}Ag_4Mo_{12}N_{16}O_{40}P$	$C_{16}H_{29}Ag_4Mo_{12}N_{12}O_{40}P$
fw	2003.50	4814.29	2587.07	2643.24
space group	*C*2/*c*	$R\bar{3}$	$P2_1/n$	$P2_1/n$
a (Å)	22.381(2)	17.6706(6)	12.1848(7)	13.755(2)
b (Å)	11.2690(7)	17.6706(6)	14.4015(8)	13.589(2)
c (Å)	19.0866(18)	23.5201(11)	13.5158(9)	14.229(2)
α (deg)	90	90	90	90
β (deg)	119.119(4)	90	91.926(3)	90.925(2)
γ (deg)	90	120	90	90
V (Å ^{3})	4205.5(6)	6360.2(4)	2370.4(2)	2659.4(7)
Z	4	3	2	2
F(000)	3760	6702	2398	2470
ρ (Mg m^{-3})	3.164	3.771	3.625	3.301
abs coeff (mm^{-1})	4.216	4.936	4.823	4.301
θ for data collection (deg)	3.29−27.48	2.18−27.48	3.02−27.48	2.08−27.49
reflns collected/unique	15 936/4810	16 630/3250	18 167/5429	20 508/6050
unique reflns (R_{int})	0.0289	0.0418	0.0438	0.0230
params	299	225	386	403
GOF on F^2	1.050	1.106	1.057	1.055
R1[a], wR2 [$I > 2\sigma(I)$]	0.0422, 0.0993	0.0402, 0.0881	0.0522, 0.1040	0.0367, 0.0889
R1, wR2 (all data)	0.0539, 0.1075	0.0446, 0.0907	0.0651, 0.1125	0.0436, 0.0940

	5	**6**	**7**	**8**
empirical formula	$C_8H_{12}Ag_4Mo_8N_{12}O_{26}$	$C_8H_{16}Ag_4Mo_8N_{16}O_{26}$	$C_4H_8Ag_5Mo_8N_8O_{26}Cl$	$C_{16}H_{16}Ag_{12}Mo_8N_{24}O_{30}$
fw	1891.30	1951.37	1926.50	3086.49
space group	$P\bar{1}$	$P\bar{1}$	*C*2/*c*	$P\bar{1}$
a (Å)	7.8389(6)	8.2465(4)	14.0585(11)	9.7391(6)
b (Å)	9.9999(7)	10.8172(5)	14.8261(11)	11.0838(6)
c (Å)	11.6357(9)	10.9336(2)	14.4347(11)	13.7370(8)
α (deg)	106.6160(10)	71.101(7)	90	72.3230(10)
β (deg)	102.630(2)	82.030(10)	99.582(3)	84.3840(10)
γ (deg)	100.051(3)	87.775(10)	90	73.71(3)
V (Å ^{3})	825.00(11)	913.81(6)	2966.7(4)	1356.01(14)
Z	1	1	4	1
F(000)	876	908	3536	1420
ρ (Mg m^{-3})	5.360	3.546	4.313	3.780
abs coeff (mm^{-1})	3.807	4.848	6.678	6.103
θ for data collection (deg)	2.37−27.48	3.18−27.48	3.10−27.48	1.56−25.71
reflns collected/unique	6343/3711	6979/4098	11 292/3395	7485/5099
unique reflns (R_{int})	0.0193	0.0167	0.0307	0.0286
params	262	283	240	391
GOF on F^2	1.024	1.024	1.165	1.061
R1[a], wR2 [$I > 2\sigma(I)$]	0.0261, 0.0622	0.0316, 0.0782	0.0455, 0.1006	0.599, 0.1328
R1, wR2 (all data)	0.0307, 0.0652	0.0382, 0.0837	0.0518, 0.1050	0.0702, 0.1418

[a] $R1 = \sum(|F_o| - |F_c|)/\sum|F_o|$; $wR2 = [\sum w(F_o^2 - F_c^2)^2/\sum w(F_o^2)^2]^{0.5}$.

from $[Cu_4(datrz)_4]^{4+}$ and *β*-octamolybdate clusters,[14c] and the other is based on $[Au_9(PPh_3)_8]^{3+}$ and $[PW_{12}O_{40}]^{3-}$ clusters.[20]

Compound **2** crystallizes in the space group $R\bar{3}$ with three formula units in the unit cell. Six two-coordinated Ag(I) atoms are linked by six 3atrz ligands through N1,N2-bridging mode (Figure 2a, Ag−N = 2.132(6) and 2.123(5) Å and N−Ag−N = 168.0(2)°) to form a double calyx[3]arene-shaped hexamer, where two $[PMo_{12}O_{40}]^{3-}$ are contained as non-coordinated guest anions (Figure 2b). Two bottom-shared bowls are open in opposite directions, and because of the limited void, two α-Keggin ions have to protrude out from the cavity with a distance between two phosphrous atoms of ∼13 Å. The guest anion is a normal α-Keggin structure composed of 12 corner- or edge-sharing MoO_6 octahedra with the central phosphorus ordered and coordinated to four oxygen atoms in a tetrahedral fashion. The P−O distances are 1.531(4) and 1.529(6) Å, respectively. The Mo−O distances can be grouped into three sets: Mo−O_t (terminal) = 1.668(4)−1.685(4) Å, Mo−O_c (central) = 2.430(3)−2.435(4) Å, and Mo−O_b (bridge) = 1.852(4)−1.967(4) Å. The bond angles of Mo−O_c−Mo are in the range of 88.76(12)−89.08(12)°, and those of Mo−O_b−Mo fall into two groups: 124.9(2)−126.2(2)° in a Mo_3O_{13} triplet and 151.5(2)−152.3(2)° between two Mo_3O_{13} triplets. Although this host−guest assembly is similar to $[Cu_6(4,7\text{-phenanthroline})_8$-

(20) Scheulz-Dobrick, M.; Jansen, M. *Eur. J. Inorg. Chem.* **2006**, 4498.

Table 2. Selected Bond Lengths (Å) and Angles (deg) and Summary of Structural Characteristics of Compounds **1**−**8**

coordination geometry of Ag	Ag−X (Å, X = N/O/Cl)	X−Ag−X (deg, X = N/O/Cl)	Ag−triazolate	POMs	assembly mode
		$[Ag_4(dmtrz)_4][Mo_8O_{26}]$ **(1)**			
linear, {N_2} (×3)	2.195(4), 2.186(4) 2.130(4), 2.135(4)	140.7(2), 138.4(2) 167.0(18)	tetranuclear cluster	β-$[Mo_8O_{26}]^{4-}$	0-D + 0-D
		$[Ag_6(3atrz)_6][PMo_{12}O_{40}]_2{\cdot}H_2O$ **(2)**			
linear, {N_2} (×6)	2.132(6), 2.123(5)	168.0(2)	hexanuclear cluster	α-$[PMo_{12}O_{40}]^{3-}$	0-D + 0-D
		$[Ag_2(3atrz)_2]_2[HPMo^{VI}_{10}Mo^{V}_{2}O_{40}]$ **(3)**			
linear, {N_2} (×2)	2.125(7), 2.103(8) 2.129(7), 2.123(7)	172.8(3), 158.3(3)	helix chain	α-$[HPMo^{VI}_{10}Mo^{V}_{2}O_{40}]^{4-}$	1-D + 0-D
		$[Ag_2(dmtrz)_2]_2[HPMo^{VI}_{10}Mo^{V}_{2}O_{40}]$ **(4)**			
linear, {N_2} (×2)	2.135(5), 2.166(5) 2.158(5), 2.158(4)	153.33(19), 151.71(17)	helix chain	α-$[HPMo^{VI}_{10}Mo^{V}_{2}O_{40}]^{4-}$	1-D + 0-D
		$[Ag_2(trz)_2]_2[Mo_8O_{26}]$ **(5)**			
linear, {N_2} (× 2)	2.130(4), 2.132(3) 2.184(3), 2.200(3)	175.39(14), 170.70(15)	zigzag chain	$[\gamma$-$Mo_8O_{26}]_n^{4n-}$ (1-D)	1-D + 1-D
		$[Ag_2(3atrz)_2][Ag_2(3atrz)_2(Mo_8O_{26})]$ **(6)**			
linear, {N_2} (×2)	2.205(4), 2.120(4)	180.0(2), 180.000(1)	zigzag chain	$[Ag_2(3atrz)_2(\gamma$-$Mo_8O_{26})]_n^{2n-}$ (2-D)	1-D + 2-D
tetrahedral {N_2O_2} (× 2)	2.181(4), 2.210(5) 2.411(3), 2.578(4)	128.21(16), 128.40(16) 95.26(14), 85.29(14) 120.88(15), 95.44(11)			
		$[Ag_4(4atrz)_2Cl][Ag(Mo_8O_{26})]$ **(7)**			
linear, {NCl} (× 2)	2.163(6), 2.435(2)	174.06(17)	looped chain	$[Ag(\beta$-$Mo_8O_{26})]_n^{3n-}$(1-D)	1-D + 1-D
linear, {N_2} (× 2)	2.164(6), 2.225(6)	171.9(2)			
quadrangular plane {O_4} (×1)	2.355(6), 2.423(6) 2.444(6), 2.451(6)	163.35(8), 80.24(19) 97.30(19), 98.9(2) 78.77(19), 163.67(8)			
		$[Ag_5(trz)_4]_2[Ag_2(Mo_8O_{26})]{\cdot}4H_2O$ **(8)**			
linear, {N_2} (×5)	2.085(12), 2.094(1) 2.106(11), 2.124(11) 2.107(11), 2.117(12) 2.085(12), 2.086(11) 2.100(12), 2.110(11)	170.2(5), 167.9(5) 165.2(5), 174.5(5) 173.4(5)	helix chain	$[Ag_2(\gamma$-$Mo_8O_{26})]_n^{2n-}$ (1-D)	3-D framework
tetrahedral, {NO_3} (×2)	2.165(11), 2.356(10) 2.367(9), 2.510(9)	139.4(4), 130.5(4) 80.5(3), 111.4(4) 85.4(3), 96.3(3)			

$(MeCN)_4]$ $[PM_{12}O_{40}]_2$ (M = Mo or W),[7d] reported by Keller and co-workers, compound **2** itself is still of interest with respect to the following aspects: (i) As far as we know, no hexanuclear Ag(I) clusters based on triazole ligands have been reported to date in the coordination chemistry of 1,2,4-triazole and its derivatives. (ii) This Ag-based metallacalix-[3]arene-shaped receptor is unique in the host−guest chemistry. To our knowledge, only a few metallacalic[3]arenes of Pt^{II} and Pb^{II} have been described, and most of the encapsulated guests are inorganic ions such as BF_4^-, NO_3^-, PF_6^-, ClO_4^-, etc.[21] (iii) Although POM-based hybrid solids have been extensively investigated, no supramolecular host−guest compounds between polynuclear silver clusters and polyoxometalate has been reported to date. As shown in

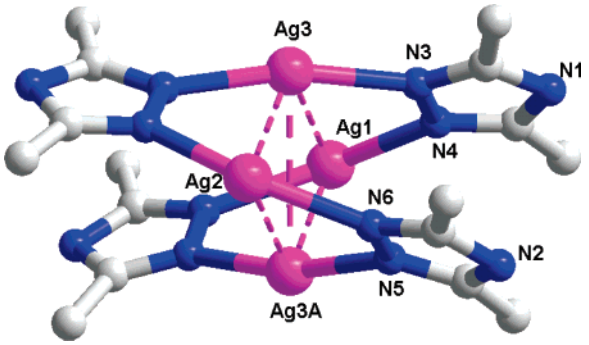

Figure 1. Structure of the tetranuclear cluster in compound **1**.

Table 3. Hydrogen-Bonding Parameters in Compounds **1**−**7**[a]

	D−H···A	*d*(D−H) (Å)	*d*(H···A) (Å)	*d*(D···A) (Å)	∠(DHA) (deg)
1	N(2)−H(2A)···O(9)^{i}	0.86	2.12	2.934(5)	158.1
	C(1)−H(1B)···O(8)^{ii}	0.93	2.28	3.235(8)	172.4
	C(3)−H(3C)···O(13)	0.93	2.47	3.297(8)	144.4
	C(5)−H(5A)···O(3)^{iii}	0.93	2.32	3.243(8)	160.3
	C(6)−H(6A)···O(2)^{iv}	0.93	2.40	3.325(7)	162.2
2	N(1)−H(1A)···O(7)^{i}	0.86	2.31	2.994(7)	136.6
	N(4)−H(4A)···O(4)^{ii}	0.86	2.26	3.016(8)	146.1
	N(4)−H(4B)···O(7)^{i}	0.86	2.23	2.979(7)	146.2
3	N(5)−H(5A)···O(18)	0.86	2.27	3.047(12)	151.1
	N(5)−H(5B)···O(7)^{i}	0.86	2.34	3.004(11)	133.7
	N(7)−H(7B)···O(3)^{ii}	0.86	2.28	3.063(12)	151.0
	C(4)−H(4A)···O(13)^{iii}	0.93	2.46	3.171(11)	133.0
4	N(4)−H(4D)···O(11)^{i}	0.86	2.23	3.043(7)	156.5
	N(5)−H(5D)···O(11)^{ii}	0.86	2.37	3.128(10)	147.3
	C(1)−H(1A)···O(19)^{iii}	0.93	2.38	3.190(7)	141.2
	C(4)−H(4C)···O(8)^{iv}	0.93	2.33	3.222(9)	154.5
5	N(5)−H(5A)···O(12)^{i}	0.86	1.85	2.690(4)	165.6
	N(6)−H(6A)···O(9)^{ii}	0.86	1.93	2.774(4)	167.8
	C(1)−H(1A)···O(4)^{iii}	0.93	2.25	3.091(5)	149.3
	C(2)−H(2A)···O(8)^{iv}	0.93	2.35	3.212(5)	154.5
	C(3)−H(3A)···O(5)^{i}	0.93	2.39	3.091(5)	131.8
	C(4)−H(4A)···O(2)	0.93	2.51	3.144(5)	126.0
6	N(2)−H(2A)···O(3)^{i}	0.86	2.22	2.863(6)	131.6
	N(5)−H(5A)···O(7)^{ii}	0.86	1.91	2.757(5)	169.1
	N(6)−H(6A)···O(12)	0.86	2.21	3.041(6)	161.6
	N(8)−H(8A)···O(9)^{iii}	0.86	2.12	2.978(6)	173.1
	C(4)−H(4A)···O(1)^{iv}	0.93	2.54	3.195(6)	128.2
7	N(3)−H(3A)···Cl(1)^{i}	0.86	2.64	3.395(6)	146.8
	C(1)−H(1A)···O(6)^{ii}	0.93	2.23	3.148(9)	167.1

[a] Symmetry coordinates for **1**: (i) $-x, -y, -z+1$; (ii) $x, y-1, z$; (iii) $-x, y-1, -z+1/2$; (iv) $-x+1/2, -y+1/2, -z+1$. For **2**: (i) $-x+1, -y, -z-1$; (ii) $x-y-1/3, x-2/3, -z-2/3$). For **3**: (i) $x-1/2, -y+3/2, z-1/2$); (ii) $-x, -y+1, -z+2$; (iii) $-x-1/2, y-1/2, -z+3/2$. For **4**: (i) $-x+1/2, y+1/2, -z-1/2$; (ii) $x+1/2, -y+5/2, z+1/2$; (iii) $-x+1, -y+3, -z-1$; (iv) $-x+3/2, y+1/2, -z-1/2$). For **5**: (i) $-x+1, -y+2, -z$; (ii) $-x+1, -y+1, -z$; (iii) $x-1, y, z-1$); (iv) $(-x+2, -y+2, -z+1)$. For **6**: (i) $-x+2, -y+2, -z-1$; (ii) $x, y, z+1$; (iii) $-x+3, -y+3, -z$; (iv) $-x+2, -y+2, -z$. For **7**: (i) $x+1/2, y-1/2, z$; (ii) $-x+2, -y+1, -z$.

Figure 2c, the host metal−organic cations and guest $[PMo_{12}O_{40}]^{3-}$ ions form three-dimensional supramolecular network through weak N−H···O hydrogen bonds (see Table 3). When the guest polyanions are removed, the Ag-trz coordination fragments present 1-D honeycomb tubular channels along the *c* axis, just like the exceptionally stable coordination polymer [ZnF(3atrz)]·solvents.[22] As depicted

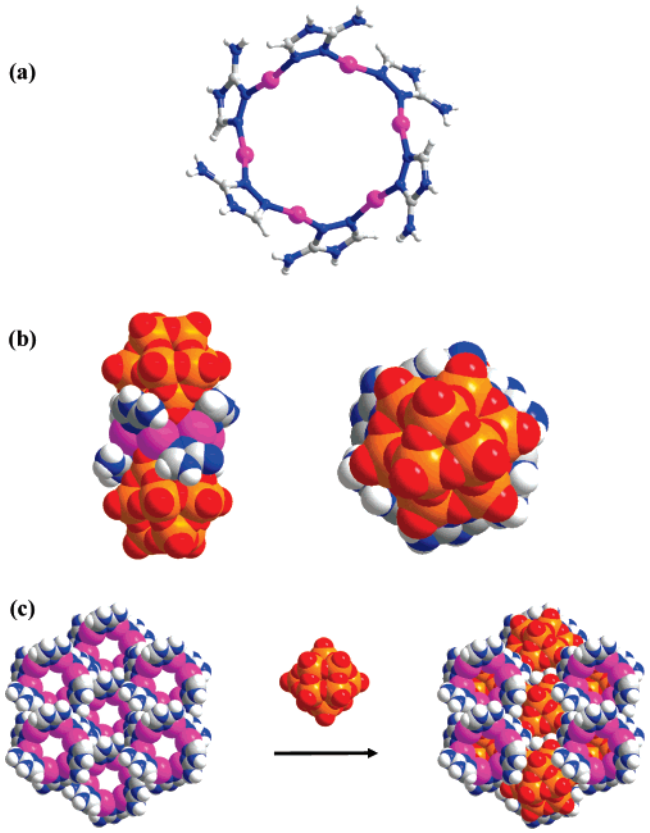

Figure 2. (a) Structure of the hexanuclear cluster in compound **2**. (b) Space-filling side (left) and top (right) views of the two polyoxometalate anions in the two bow-shaped cavities of the hexamer. (c) 1-D honeycomb tubular channels formed by silver clusters (left) and 3-D hybrid supramolecular architecture (right) viewed along the *c*-axis.

in Figure S2, each hexanuclear cyclic unit is linked by twelve Keggin anions via hydrogen bonds with center-to-center distances of about 10.28 and 13.67 Å. On the other hand, Keggin anions are connected by six hexanuclear clusters. Therefore, the overall 3-D packing framework of **2** can be rationalized as a 6,12-connected net by assignment of the $[Ag_6(3atrz)_6]^{6+}$ rings as 12-connected nodes, the $[PM_{12}O_{40}]^{3-}$ clusters as six-connected nodes, and the weak hydrogen bonds as linkers.

Compounds **3** and **4** crystallize isostructurally consisting of one-dimensional Ag−1,2,4-triazolate helix chains and Keggin anions. The metal−organic helix chains contain two crystallographically unique silver ions linked by two organic ligands through N1,N2- and N1,N4-bridging modes (Figure 3a). The long pitches of the helix chains in **3** and **4** along the *c*-axis are 17.891(31) and 19.950(21) Å, respectively. Both silver atoms are of linear geometry with Ag−N distances falling in the range of 2.103(8)−2.158(5) Å. The corresponding N−Ag−N angles are 158.3(3) and 172.8(3)° for **3** and 153.33(19) and 151.71(17)° for **4**. It should be pointed out that because of the symmetrical structures of 1,2,4-triazole or its derivatives and the diversities of their bridging modes, 2-D helical chain structures with triazole ligands are rare, and to our knowledge, only one example

(21) (a) Schnebeck, R. D.; Freisinger, E.; Lippert, B. *Angew. Chem., Int. Ed.* **1999**, *38*, 168. (b) Schnebeck, R. D.; Freisinger, E.; Glahé, F.; Lippert, B. *J. Am. Chem. Soc.* **2000**, *122*, 1381. (c) Yu, S. Y.; Huang, H.; Liu, H. B.; Chen, Z. N.; Zhang, R. B.; Fujita, M. *Angew. Chem., Int. Ed.* **2003**, *42*, 686.

(22) Su, C. Y.; Goforth, A. M.; Smith, M. D.; Pellechia, P. J.; Loye, H. C. *J. Am. Chem. Soc.* **2004**, *126*, 3576.

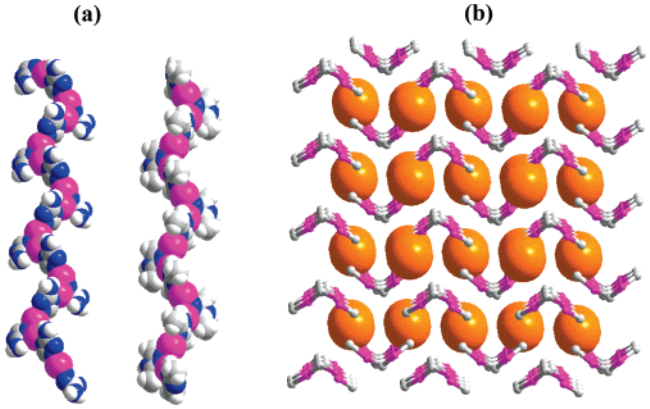

Figure 3. (a) Space-filling views of the helix chains in compounds **3** (left) and **4** (right). (b) The schematic representation of the 0-D + 1-D supramolecular assembly. The Keggin POM anions are represented as orange spheres.

of a single-stranded 4_1 helix has been reported.[23] Moreover, pyrazole-like and imidazole-like bridging modes of triazole ligands have never been observed in the same structure to link metal centers. The polyoxoanion $[HPMo^{VI}_{10}Mo^{V}_{2}O_{40}]^{4-}$ in **3** and **4** exhibits a distorted α-Keggin structure with center P atom surrounded by a cube of eight half-occupied oxygen atoms. P−O bonds range from 1.481(6) to 1.592(9) Å. This structure feature often appears in $[XMo_{12}O_{40}]^{n-}$ with the α-Keggin structure, which has been explained by several groups.[24] Three sets of Mo−O distances are Mo−O(t) = 1.644(6)−1.668(4) Å, Mo−O(b) = 1.810(7)−2.000(7) Å, and Mo−O(c) = 2.408(10)−2.522(6) Å. The helices and Keggin anions are linked by complex hydrogen bonds (N−H···O or C−H···O) to generate a three-dimensional inorganic−organic hybrid supramolecular structure (Figure S3). The distances between the N or C atoms of organic ligands and oxygen atoms of the POM anions range from 3.004(11) to 3.222(9) Å. The whole packing schemes of compounds **3** and **4** present layer structures (Figure 3b) following the pattern ···ABAB··· (A = POM layer and B = Ag-trz layer) along the *a*-axis. The B layers are parallel to each other along the *a*-axis with a distance between the planes of two triazole rings of about 12 Å, which is slightly longer than the diameter of POM anions (∼10 Å).

The supramolecular structure of **5** consists of pairs of $[Ag_2(trz)_2]_n^{2n+}$ zigzag chains and one $[Mo_8O_{26}]_n^{4n-}$ chain. Two crystallographically unique silver ions are linked by trz ligands through the N1,N4-bridging mode to generate a 1-D zigzag chain (Figure 4a). Both silver atoms are of linear geometry with Ag−N distances falling in the range of 2.130(4)−2.200(3) Å and N−Ag−N angles of 170.70(15) and 175.39(14)°. Each molybdenum atom of the polyoxometalate chain attains a distorted octahedral environment by coordination of six oxygen atoms. The four asymmetric $[MoO_6]$ octahedra connected through their edges to form the $[Mo_4O_{13}]^{2-}$ unit, which are further stacked together by edge-sharing to give rise to γ-$[Mo_8O_{26}]^{4-}$ octamolybdate clusters. The γ-octamolybdate units are linked together through sharing common vertices to form infinite chain along the *a*-axis (Figure 4b). In the solid state of **5**, two types of 1-D chains are held together and extended to a 3-D framework via strong N−H···O and weak C−H···O hydrogen bonding (Figure S4). One non-coordinated nitrogen atom and two carbon atoms of the organic ligands all participate in hydrogen bonding with terminal oxo atoms of the POM chain (See Table 3). As shown schematically in Figure 4c, the overall 3-D framework of **5** also presents layer structures following the pattern ···ABAB··· along the *b*-axis. Two types of chains are basically vertical to each other, and they extend along the *a*- and *c*-axes.

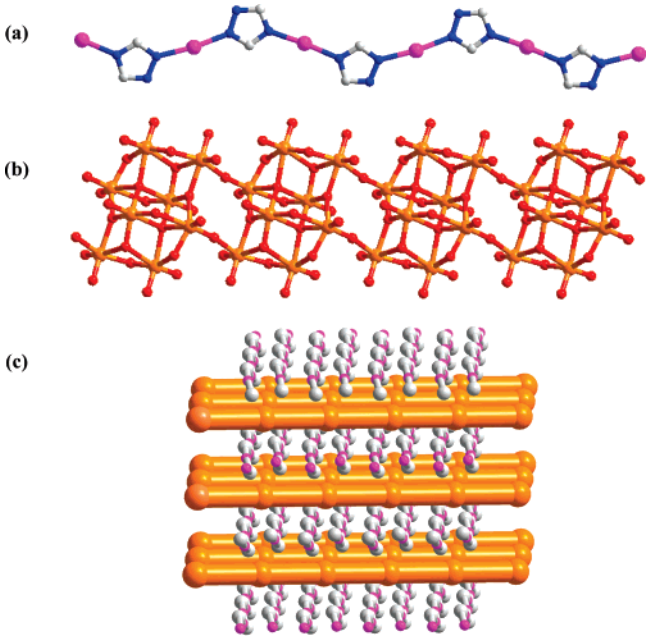

Figure 4. (a) Zigzag Ag-triazolate chain in compound **5**. (b) 1-D inorganic $[Mo_8O_{26}]_n^{4n-}$ constructed from the γ-$[Mo_8O_{26}]$ cluster through sharing common vertices. (c) schematic representation of the 1-D + 1-D hybrid assembly.

X-ray diffraction analysis reveals that **6** is composed of anionic $[Ag_2(3atrz)_2(Mo_8O_{26})]_n^{2n-}$ two-dimensional netlike frameworks penetrated by cationic $[Ag_2(3atrz)_2]_n^{2n+}$ zigzag chains. Although numerous types of entanglements of multiple motifs in coordination polymeric networks have been reviewed,[25] examples of threading 1-D chains into 2-D sheets are relatively rare.[26] The 1-D $[Ag_2(3atrz)_2]_n^{2n+}$ zigzag chain is similar to the $[Ag_2(trz)_2]_n^{2n+}$ chain in compound **5**. The two unique silver atoms are both of linear geometry (Ag−N = 2.205(4) and 2.120(4) Å) and are connected by the 3atrz ligands using an imidazole-like bridging mode (Figure 5a). The 2-D $[Ag_2(3atrz)_2(Mo_8O_{26})]_n^{2n-}$ framework

(23) Zhang, J. P.; Lin, Y. Y.; Huang, X. C.; Chen, X. M. *Chem. Commun.* **2005**, 1258.
(24) (a) Attanasio, D.; Bonamicao, M.; Fares, V.; Imeratori, P.; Suber, L. *Dalton Trans.* **1990**, 3221. (b) Maguerès, P. L.; Ouahab, L.; Golhen, D.; Grandjean, D.; Pena, O.; Jegaden, J. C.; Gomez-Garcia, C. J.; Delhaès, P. *Inorg. Chem.* **1994**, *33*, 5180. (c) Neier, R.; Trojanowaki, C.; Mattes, R. *Dalton Trans.* **1995**, 1308. (d) Fender, N. S.; Kahwa, I. A.; White, A. J. P.; Williams, D. J. *Dalton Trans.* **1998**, 1729.
(25) Carlucci, L.; Ciani, C.; Proserpio, D. M. *Coord. Chem. Rev.* **2003**, *246*, 247.
(26) (a) Sharma, C. V. K.; Rogers, R. D. *Chem. Commun.* **1999**, 83. (b) Tong, M. L.; Wu, Y. M.; Ru, J.; Chen, X. M.; Chang, H. C.; Kitagawa, S. *Inorg. Chem.* **2002**, *41*, 4846. (c) Zaman, M. B.; Smith, M. D.; zur Loye, H. C. *Chem. Commun.* **2001**, 2256. (d) Liao, J. H.; Juang, J. S.; Lai, Y. C. *Cryst. Growth Des.* **2006**, *6*, 354.

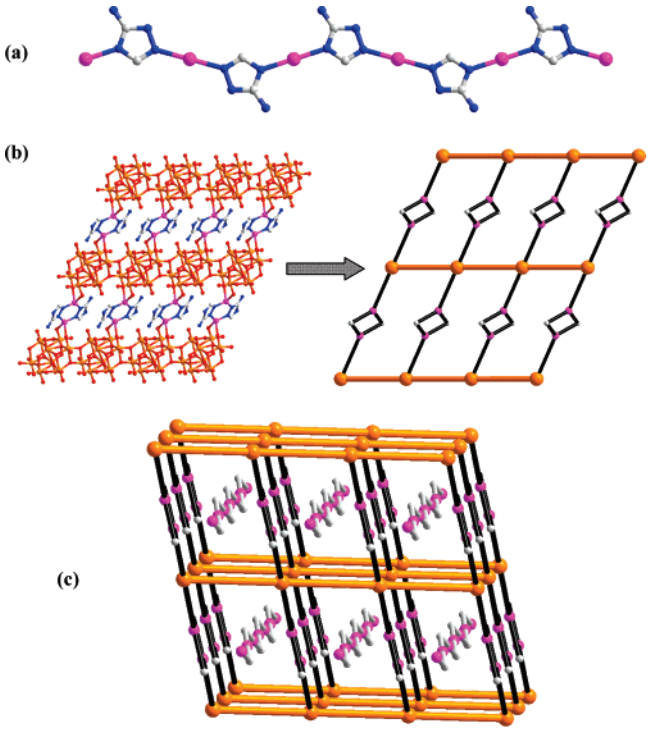

Figure 5. (a) 1-D zigzag metal-organic chain in **6**. (b) 2-D $[Ag_2(3atrz)_2(Mo_8O_{26})]_n^{2n-}$ hybrid layer (left) and its topological representation (right). (c) Schematic representation of the 1-D in 2-D supramolecular assembly of **6**.

is constructed from 1-D $[Mo_8O_{26}]_n^{4n-}$ chains and $[Ag_2(3atrz)_2]^{2+}$ binuclear units. Similar to compound **5**, the basic polyoxometalate building block is also the γ-isomer of $[Mo_8O_{26}]^{4-}$ when the oxygen atoms donated by adjacent octamolybdate subunits are removed. However, the two adjacent subunits are linked not through sharing common vertices as in **5** but through common edges (Figure S5). Therefore, the molybdate ribbon may be regarded as being constructed of octamolybdate units joined at two oxo-groups or from two groups of cis-edge-sharing tetranuclear units united through edge-sharing. Similar octamolybdate chains have been found in $K_2Mo_4O_{13}$,[27] $[(C_5H_7N_2)_2Mo_4O_{13}]$,[28] $[Cu(Hdipyreth)Mo_4O_{13}]$,[29] $[Cu(bpy)Mo_4O_{13}]$,[30] and $[Cu_2(4PBIM)_2Mo_4O_{13}]$.[31] In the $[Ag_2(3atrz)_2]^{2+}$ binuclear units, two silver atoms are linked by two 3atrz ligands through a pyrazole-like bridging mode, which makes the distance between two silver atoms 3.337(24) Å. Each γ-$[Mo_8O_{26}]^{4-}$ cluster in the inorganic chains uses two opposite pairs of oxo groups of adjacent MoO_6 octahedra to coordinate two Ag^+ ions, that is, to connect two binuclear units to form the 2-D network. Thus, each silver atom links two nitrogen atoms and two terminal oxygen atoms (Ag−N = 2.181(4) and 2.210(5) Å, Ag−O = 2.411(3) and 2.578(4) Å) to form a distorted tetrahedral environment. As depicted in Figure 5b, the overall 1-D hybrid layer can be rationalized as a novel 3,4-connected net when silver atoms and octamolybdates are regarded three- and four-connected nodes, respectively. If the dinuclear $[Ag_2(3atrz)_2]^{2+}$ subunits are further simplified as linkers, this 2-D network has a much simpler (4,4) topology with parallelogram grids of 8.25 × 14.49 Å. Further, the $[Ag_2(3atrz)_2]_n^{2n+}$ infinite chains penetrate into the $[Ag_2(3atrz)_2(Mo_8O_{26})]_n^{2n-}$ sheets to give the 1-D in 2-D supramolecular structure of compound **6**. The spacing of the two parallel sheets is 12.75 Å. This supramolecular assembly is further stabilized by non-classic N···O and C···O hydrogen bonding between nitrogen or carbon atoms of 3atrz ligands in the 1-D chains and oxygen atoms of the octamolybdate clusters in the 2-D grids (Figure S6). Moreover, there is also N···O hydrogen bonding between the binuclear units and POM clusters in the 2-D grids. The overall supramolecular architecture of rods in grids is simply shown schematically in Figure 5c, which is intriguing in the area of chemical topological. To the best of our knowledge, only one 1-D-in-2-D entangled system incorporating polyoxometalates has been reported to date.[26d]

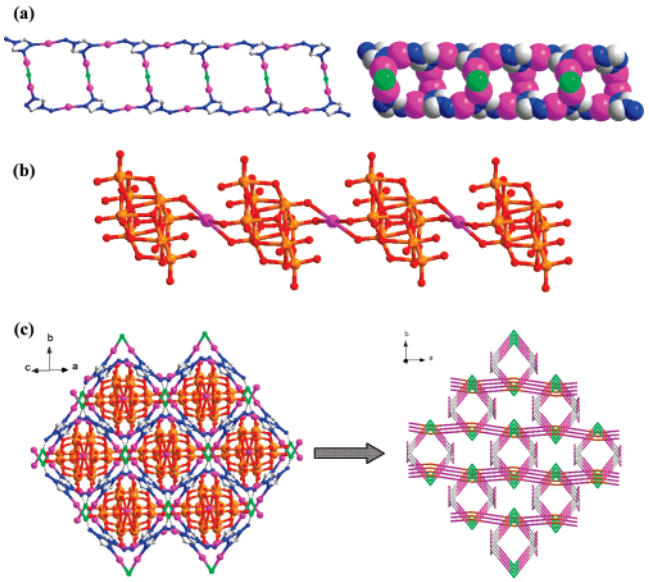

Figure 6. (a) Ball and stick (left) and space-filling (right) representations of the looped chain in compound **7**. (b) Inorganic $[AgMo_8O_{26}]_n^{3n-}$ chain in **7**. (c) Overall supramolecular assembly between two kinds of chains (left) and the topological representation (right).

Complex **7** consists of interesting cationic $[Ag_4(4atrz)_2Cl]_n^{3n+}$ looped chains (Figure 6a) and unprecedented anionic $[Ag(Mo_8O_{26})]_n^{3n-}$ chains (Figure 6b). The two unique silver atoms in the cationic chain are both of linear coordination geometry. Each 4atrz ligand links two Ag^+ ions through the N1 (or N2) atom (Ag(2)−N(2) = 2.164(6) Å) and the amino group (Ag(2)−N(3) = 2.225(6) Å) to give a 1-D single-chain structure. Then, two single chains were connected by $[Ag_2Cl]^+$ units (Ag(1)−Cl(1) = 2.435(2) Å) through the uncoordinated N2 (or N1) atoms of the triazole ligands (Ag(1)−N(1) = 2.163(6)) to generate an interesting looped chain structure. The $[Ag_2Cl]^+$ units locate alternately at both sides of the chain. Notably, this is the first example in the coordination chemistry of 4-amino-1,2,4-triazole ligands in which an amino group participates in bonding. Moreover, the Ag−N bond distance (2.225(6) Å) is distinctly longer than those between Ag^+ ions and the nitrogen atoms of

(27) Gatehouse, B. M.; Leverett, P. *J. Chem. Soc. A* **1971**, 2107.
(28) Pavani, K.; Ramanan, A. *Eur. J. Inorg. Chem.* **2005**, 3080.
(29) Rarig, R. S., Jr.; Zubieta, J. *Polyhedron* **2003**, *22*, 177.
(30) Rarig, R. S., Jr.; Hamela, P. J.; Zubieta, J. *Solid State Sci.* **2002**, *4*, 77.
(31) Chen, L. J.; He, X.; Xia, C. K.; Zhang, Q. Z.; Chen, J. T.; Yang, W. B.; Lu, C. Z. *Cryst. Growth Des.* **2006**, *6*, 2076.

triazole ring (2.164(6) and 2.163(6) Å). On the other hand, this metal−organic chain can also be regarded as $[Ag_6(4atrz)_4Cl_2]$ hexanuclear rings linked each other to form extended structure. Further, the cationic $[Ag_4(4atrz)_2Cl]_n^{3n+}$ units are linked through N−H···Cl hydrogen binding to give a three-dimensional supramolecular porous framework (Figure S7). The 1-D channels formed possess dimensions of about 9.28 × 9.06 Å, which are perfectly occupied by the inorganic chains. The anionic $[Ag(Mo_8O_{26})]_n^{3n-}$ chain in **7** is constructed from the β-octamolybdate clusters and single-coordinated electrophilic silver ions. The Ag^+ ion is sandwiched between two β-octamolybdate units. Each β-Mo_8O_{26} unit forms covalent interactions with two silver atoms through four terminal oxygen atoms of two $\{Mo_4O_{13}\}$ subunits with the Ag−O distances range from 2.355(6) to 2.451(6) Å and the O−Ag−O angles range from 80.24(19) to 163.67(8)°. Each four-coordinated Ag(I) ion is of a slightly distorted quadrangular plane. The distance between two adjacent silver atom is 9.198(16) Å. Although a large number of hybrid materials based on octamolybdate and its analogous compounds have been reported, such a one-dimensional infinite chain structure constructed by $[Mo_8O_{26}]^{4-}$ building blocks linked only by single Ag^+ ions is the first example. The overall 3-D suparmolecular assembly is further stabilized by C−H···O hydrogen bonding between the carbon atoms of 4atrz ligands and terminal oxygen atoms of octamolybdate clusters. The whole 1-D + 1-D supramolecular architecture of compound **7** is simply illustrated in Figure 6c and is completely novel to our knowledge.

Compound **8** is constructed from 1-D $[Ag_2(Mo_8O_{26})]_n^{2n-}$ anionic chains, integrated by pairs of $[Ag_5(trz)_4]_n^{n-}$ chains into a 3-D framework. As shown in Figure 7a, there are six crystallographically independent silver(I) centers, which have two kinds of coordination environments with the Ag(2) center being four-coordinated and other silver centers being two-coordinated. Linear coordinated Ag(1), Ag(4), and Ag(5) are linked by three triazole ligands through a pyrazole-like bridging mode to give $[Ag_3(trz)_3]$ neutral trigonal units. The Ag−N bond distances and N−Ag−N angles are 2.085(12)−2.117(12) Å and 165.2(5)−174.5(5)°, respectively. The Ag···Ag distances in this trigonal unit are 3.603(2), 3.609(2), and 3.801(2) Å. Three triazole rings all deviate slightly from the trigonal plane formed by three silver atoms to ease the repulsion of metal ions, and the dihedral angles are about 6.5, 15.9, and 19.4°, respectively. Although $[Cu_3(trz)_3]$ subunits have been reported to construct coordination polymers,[13e] $[Ag_3(trz)_3]$ in **8** is the first structurally characterized cyclic trinuclear example with silver centers. This unique $[Ag_3(trz)_3]$ unit is further connected by another two linear silver ions (Ag(3) and Ag(6)) and one triazole ligands (imidazole-like linking mode) to give a 1-D chain depicted in Figure 7b. In the inorganic chain, the octamolybdate cluster contains 14 μ_t-O, six μ_2-O, four μ_3-O, and two μ_4-O and is a γ−isomer like that in compounds **5** and **6**. Each γ−Mo_8O_{26} unit forms covalent interactions with four silver atoms (Ag(2)) through four μ_t-O and two μ_2-O of two $\{Mo_4O_{13}\}$ subunits (Figure 7c). Thus, the Ag^+ ions are sandwiched between two octamolybdate units. Each four-coordinated Ag(I) ion is not of quadrangular plane geometry as in the reported $[Ag_2(Mo_8O_{26})]^{2-}$ examples[10f,10j] but has a distorted tetrahedral geometry coordinated to three oxygen atoms and one nitrogen atoms (N(10)). The Ag−O and Ag−N distances are 2.356(10)−2.510(9) and 2.165(11) Å, respectively. The N−Ag−O and O−Ag−O angles are 111.4(4)−139.4(4) and 80.5(3)−96.3(3)°, respectively. The distance between two silver atoms is 4.911(2) Å. Moreover, the Mo(4) atom in the $\{Mo_4O_{13}\}$ subunit is coordinated to N(12) atom with an Mo−N distance of 2.236(11) Å. Thus, two non-coordinated nitrogen atoms (N(10) and N(12)) of triazole ligands in the meta−-organic fragments covalently link the inorganic $[Ag_2Mo_8O_{26}]_n^{2n-}$ chains to give the unique 3-D organic−inorganic hybrid frameworks of compound **8** (Figures 7d and S8). To the best of our knowledge, only limited discrete $[Ag_2Mo_8O_{26}]_n^{2n-}$ chains have been reported by our and other groups to date,[10f,10j] and compound **8** is the first highly dimensional architecture which uses $[Ag_2Mo_8O_{26}]_n^{2n-}$ as building blocks. The topological representation of the overall networks is depicted in Figure 7d, which can be described as a 3-D framework based on two kinds of 1-D rod-shaped subunits according to the principles of rod-packing.

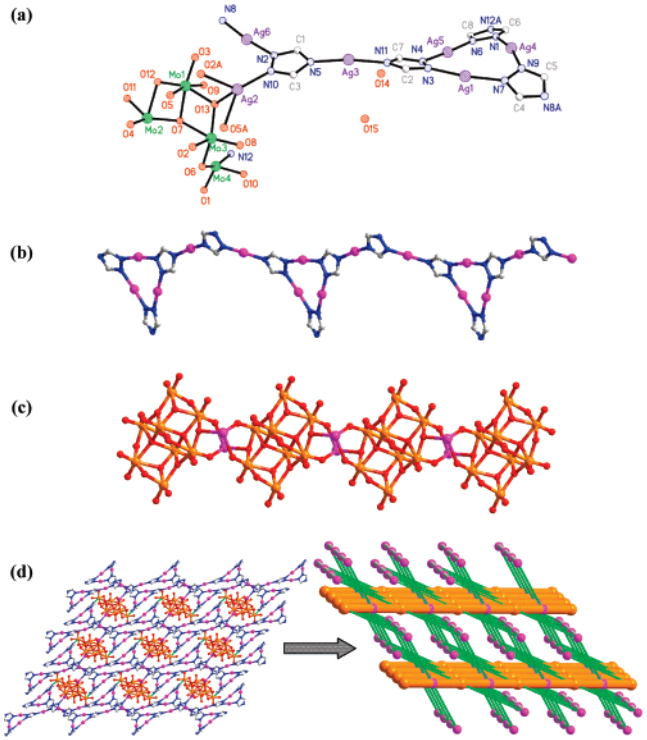

Figure 7. (a) ORTEP diagram of compound **8** showing the local coordination environment in the asymmetric unit and 30% thermal ellipsoids. (b) 1-D helix Ag-triazolate chain. (c) 1-D inorganic $[Ag_2Mo_8O_{26}]_n^{2n-}$ chain. (b) 3-D framework of compound **8** (left) and its topological representation based on two kinds of rod-shaped building units (right).

Spectroscopic Characterizations. FT-IR and ESR. In the FT-IR spectra (Figure S9) of compounds **1**−**8**, the peaks between 600 and 1100 cm^{-1} are attributed to the octamolybdate or Keggin ions, and the peaks in the range of 1000−1700 cm^{-1} and 3200−3500 cm^{-1} are from the 1,2,4-triazole ligands and lattice water molecules. The peak positions corresponding the Keggin anions differed slightly from those

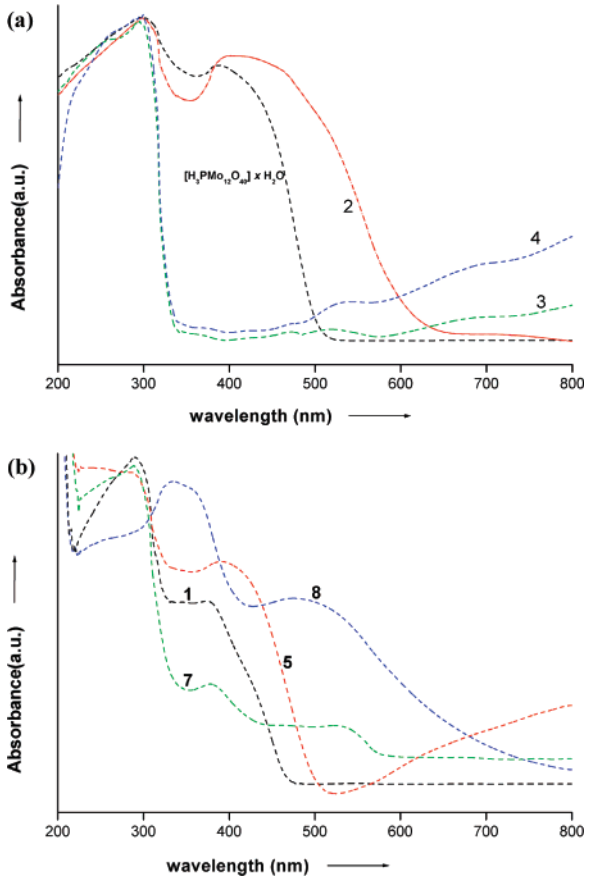

Figure 8. UV−vis absorption spectra of $H_3[PMo_{12}O_{40}]\cdot xH_2O$ and compounds **1**−**8**.

of the original acids, as observed for other organic−inorganic hybrids containing charge-compensating organics or transition metal coordination fragments and Keggin ions.[7f,7g,32] The ESR spectra for compounds **2**, **3**, and **4** (Figure S10) are recorded on polycrystalline samples at room temperature. The results show that compound **2** is ESR silent, and the spectra of **3** and **4** are typical of Mo^{5+} ions, which were consistent with the results of the X-ray analysis. The following parameters are obtained: $g = 1.9327$ for **3** and $g = 1.9374$ for **4**.

UV−vis Absorption Spectra. The UV−vis absorption spectra of these hybrid supramolecular compounds, between 200 and 800 nm, are presented in Figure 8. For comparison, the spectrum of $H_3[PMo_{12}O_{40}]\cdot xH_2O$ is also investigated under the same conditions. As shown in Figure 8a, the absorption spectra of compounds **2**−**4** and phosphordodecamolybdates all present one bond centered around 300 nm, which is a characteristic bond of heteropolyacids attributed to the O → Mo LMCT.[33] Shoulder bonds are observed for $H_3[PMo_{12}O_{40}]\cdot xH_2O$ and compound **2** with absorption peaks at 380 and 402 nm, respectively. The $H_3[PMo_{12}O_{40}]\cdot xH_2O$ is transparent at $\lambda > 530$ nm. In contrast, hybrid solid **2** shows new absorption up to $\lambda_o = 660$ nm (λ_o is the value at which the absorbance reach the baseline value). The red-shifted λ_o accompanied the increase in the reduction potential of the POM acceptors, as observed for other charge-transfer salts. In accord with the Mulliken theory,[34] the new (visible) absorption bands were ascribed to intense charge transfer between the host $[Ag_6(3atrz)_6]^{3+}$ fragments and the guest $[PMo_{12}O_{40}]^{3-}$ in complex **2**. To the best of our knowledge, hybrid supramolecular compound **2** is the first charge-transfer salt in the M′/ligands/ POM hybrid family identified by the UV−vis spectroscopy. This charge-transfer character is also confirmed by the crystal color change ($H_3[PMo_{12}O_{40}]\cdot xH_2O$, yellow → **2**, orange). In the case of compounds **3** and **4**, the blue shift of λ_o to ∼350 nm is caused by the reduction of α-Keggin ions under hydrothermal conditions. The black crystal color of these two compounds is in accordance with this result. The absorption spectra of these compounds based on the octamolybdate cluster (**1**, **5**, **7**, and **8)** are given in Figure 8b. The absorption bonds in the UV range of the spectra for compounds **1**, **5**, and **7** at 290 nm were assigned to a charge-transfer transition from the terminal oxygen nonbonding π-type HOMO to the molybdenum π-type LUMO,[35] which is shifted by about 45 nm in compound **8** (335 nm). This red shift maybe attributed to two aspects: one is that **8** is not supramolecular architecture like **1**, **5**, and **7** but instead is a three-dimensional frameworks, and the other is the formation of Mo−N bonds in this compound.[35,36] A little absorption in the visible range is consistent with the color of these compounds.

Study of Optical Band Gap. Several examples have shown that POM-based inorganic−organic hybrids are semiconductors. To explore the conductivity of compounds **1**−**8**, the measurements of diffuse reflectivity for powdered crystal samples were used to obtain their band gap (E_g). The band gap, E_g, was determined as the intersection point between the energy axis and the line extrapolated from the linear portion of the absorption edge in a plot of Kubelka−Munk function F against energy E.[37,38] Kubelka−Munk function, $F = (1 - R)^2/2R$, was converted from the recorded diffuse reflectance data, where R is the reflectance of an infinitely thick layer at a given wavelength. The F versus E plots for the compounds are shown in Figure S11, and the E_g values assessed from the steep absorption edge are 2.43 eV for $H_3[PMo_{12}O_{40}]\cdot xH_2O$, 2.52 eV for **1**, 1.94 eV for **2**, 2.15 eV for **3**, 2.34 eV for **5**, 3.58 eV for **7**, and 2.27 eV for **8**, which indicate that these hybrid compounds are potential semiconductor materials. This has also been observed in several reported POM-based inorganic−organic hybrid sol-

(32) Vitoria, P.; Ugalde, M.; Gutiérrez-Zorrilla, J. M.; Román, P.; Luque, A.; Felices, L. S.; García-Tojal, J. *New J. Chem.* **2003**, *27*, 399.
(33) Zhao, S. L.; Zhang, H. H.; Huang, C. C. *Chem. J. Chin. Univ.* **2002**, *23*, 521.
(34) (a) Mulliken, R. S. *J. Am. Chem. Soc.* **1952**, *74*, 811. (b) Mulliken, R. S.; Person, W. B. *Molecular Complexes. A Lecture and Reprint Volume*; Wiley: New York, 1969. (c) Foster, R. *Organic Charge-Transfer Complexes*; Academic: New York, 1969. (d) Maguerès, P. L.; Hubig, S. M.; Lindeman, S. V.; Veya, P.; Kochi, J. K. *J. Am. Chem. Soc.* **2000**, *122*, 10073.
(35) Xia, Y.; Wu, P. F.; Wei, Y. G.; Wang, Y.; Guo, H. X. *Cryst. Growth Des.* **2006**, *6*, 253.
(36) Du, Y.; Rheingold, A. L.; Maatta, E. A. *J. Am. Chem. Soc.* **1992**, *114*, 345.
(37) Pankove, J. I. *Optical Processes in Semiconductors*; Prentice Hall: Englewood Cliffs, NJ, 1971.
(38) Wesley, W. M.; Harry, W. G. H. *Reflectance Spectroscopy*; Wiley: New York, 1966.

ids, such as $Co_2(bpy)_6(W_6O_{19})_2$ (E_g = 2.2 eV),[39] [Cd(BPE)-(α-Mo_8O_{26})][Cd(BPE)$(DMF)_4$]·2DMF (E_g = 3.45 eV),[26d] and (n-$Bu_4N)_2[Mo_6O_{17}$-(≡NAr)$_2$] (Ar = o-$CH_3OC_6H_4$) (E_g = 2.25 eV).[35] In our opinion, the discrete polyoxometalate clusters or 1-D POM chains in the hybrid structures appear to be responsible for their optical band gap. Moreover, the variety of the E_g values suggests that the optical band gap of polyoxometalates could be tuned effectively and controllably via chemical modification using suitable organic ligands.

Photoluminescence Properties. Recently, inorganic−organic hybrid solids have been investigated for fluorescence properties and for potential applications as luminescent materials, such as light-emitting diodes (LEDs).[40] Because of their ability to affect the emission wavelength and strength of organic materials, the syntheses of inorganic−organic coordination polymers or hybrids by the judicious choice of conjugated organic spacer and transition metal centers can be an efficient method to obtain new types of electroluminescent materials, especially for d^{10} or d^{10}−d^{10} systems.[41] In our previous work, we explored a series of Zn/Cd-1,2,4-triazole coordination polymers or polynuclear compounds with strong blue fluorescence.[14b] Here, we reported the luminescence properties of this novel Ag/1,2,4-triazole/polyoxometalates hybrid supramolecular family in the solid state. As shown in Figure 9a, upon excitation of these solid samples at λ = 255 nm, the main emission bands of complexes **1**−**8** and $H_3[P(Mo_3O_{10})_4]$ are located in similar positions exhibiting strong fluorescence (λ_{max} = 421 and 488 nm) with slightly different band shapes. It is clear that the polyoxometalate components should be responsible for the emissions. Because the molybdenum ions in the $[Mo_8O_{26}]^{4-}$ or $[PMo_{12}O_{40}]^{3-}$ clusters have d^0 electron configurations, these two emissions are the result the oxygen-to-metal (O → Mo) ligand-to-metal transfer ([LMCT]).[42] We tentatively assign the 421 and 488 nm emissions to be mainly originated from the O_t → Mo and μ_2-O → Mo[1][LMCT], respectively. Moreover, a series of relative weak emissions in the 525−550 nm range may be attributed to the O_c, μ_3-O, or μ_4-O → Mo[1][LMCT] transition. This assignment can be supported by the basic three sets of Mo−O bonds that exist in the polyoxometalate clusters. Searching for the Ag^I ion-based [MLCT] or [LMCT] emissions for these compounds at room temperature was further carried out. Upon excitation of these solid samples at λ = 325 ± 5 nm, a series of sharp emissions in the 435−455 nm range (λ_{max} = 448 nm for **1**, 453 nm for **2**, 447 nm for **3**, 436 nm for **4**, 439 nm for **5**, 438 nm for **7**, and 435 nm for **8**) along with O → Mo emissions were observed, except for those for $H_3[PMo_{12}O_{40}]\cdot xH_2O$ (Figure 9b). The O → Mo [LMCT] emission bonds are similar to those excited at 255 nm except that the intensity was decreased. The sharp emission bonds in the 435−455 nm

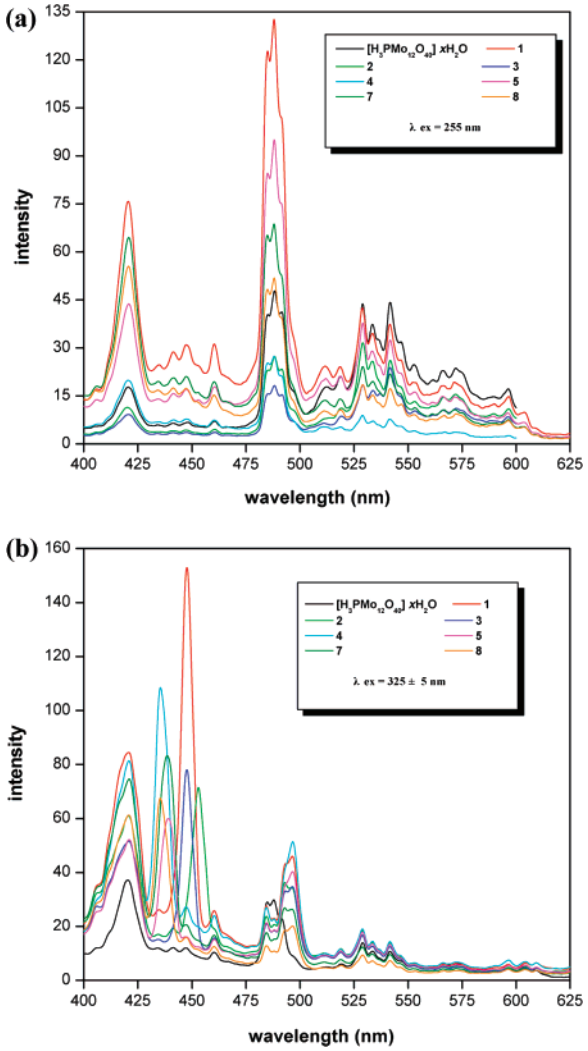

Figure 9. Emission spectra of $H_3[PMo_{12}O_{40}]\cdot xH_2O$ and compounds **1**−**8** upon excitation of these solid samples at λ = 255 (top) and 325 ± 5 nm (bottom), respectively.

range of compounds **1**−**5** and **7**−**8** are neither [MLCT] nor [LMCT] in nature and can probably be assigned to the intraligand fluorescent emissions for their sharpness and similarity to the reported intraligand [π − π*] emissions observed for the Cd/1,2,4-triazole coordination compounds.[43] The 1,2,4-triazole and the alkyl-substituted ones are not known to be strong emitters, and the [π−π*] emission peaks of these small ligands should lie in the UV region. These emissions may be red-shifted to the visible region; however, they can hardly be detected because of the strong spin-forbidden nature of the T_1 → S_0 processes. As described by Chen et al. for the photoluminescence phenomena of th e 2-D coordination polymers $[Ag(trz)]_n$,[44] the observation of emission from the 1,2,4-triazolate from these hybrid supramolecular compounds should be ascribed to the internal heavy metal effect, in which the spin-forbidden T_1 → S_0 processes become allowed by shortening of the usually very long lifetimes to milliseconds. The results demonstrated

(39) Zhang, L.; Wei, Y.; Wang, C.; Guo, H.; Wang, P. *J. Solid State Chem.* **2004**, *177*, 3433.
(40) Bunz, U. H. F. *Chem. Rev.* **2000**, *100*, 1605.
(41) (a) Seward, C.; Jia, W. L.; Wang, R. Y.; Enright, G. D.; Wang, S. N. *Angew. Chem., Int. Ed.* **2004**, *43*, 2933. (b) Yam, V. W. W.; Lo, K. K. W. *Chem. Soc. Rev.* **1999**, *28*, 323.
(42) Yamase, T. *Chem. Rev.* **1998**, *98*, 307.
(43) Ding, B.; Yi, L.; Wang, Y.; Cheng, P.; Liao, D. Z.; Yan, S. P.; Jiang, Z. H.; Song, H. B.; Wang, H. G. *Dalton Trans.* **2006**, 665.
(44) Zhang, J. P.; Lin, Y. Y.; Huang, X. C.; Chen, X. M. *J. Am. Chem. Soc.* **2005**, *127*, 5495.

again that it is a feasible strategy to enhance the phosphorescence of organic molecules via an internal heavy metal effect.[45]

Thermogravimetric Analysis (TGA). The thermal stabilities of compounds **1**−**5** and **7**−**8** were investigated on crystalline samples under an air atmosphere from 40 to 700 °C. The TG/DTA curves are provided in Figure S12. The TG curves of these compounds are similar, and all basically show one sharp stage of weight loss in the temperature range of 300−450 °C. The weight loss curve of compound **1** showed that it was stable up to ∼350 °C. Over the range of 350−435 °C, the sharp weight loss was caused by the decomposition of dmatrz ligands (exptl, 20.15%; calcd, 19.39%). The TG curve of **2** showed two stages of weight loss in the temperature range of 40−403 °C. The whole weight loss (11.02%) is in good agreement with the calculated value (10.85%) for one water molecules and six triazole ligands. The TG curves of compound **3**, **4**, **5**, **7**, and **8** were similar to that of **1**, and the sharp weight losses all correspond to the decomposition of the organic component. The detailed values of temperatures and weight losses are given in Table S1. It should be pointed out that slight weight increases are observed from the thermogravimetric curves of these compounds because the residual silver atoms were finally oxidized to Ag_2O under an air atmosphere. Similar results have been formerly observed for other compounds containing silver (I) or copper (I) atoms.[46]

(45) (a) Che, C. M.; Chao, H. Y.; Miskowski, V. M.; Li, Y. Q.; Cheung, K. K. *J. Am. Chem. Soc.* **2001**, *123*, 4985. (b) Chao, H. Y.; Lu, W.; Li, Y. Q.; Chan, M. C. W.; Che, C. M.; Cheung, K. K.; Zhu, N. Y. *J. Am. Chem. Soc.* **2002**, *124*, 14696. (c) Omary, M. A.; Rawashdeh-Omary, M. A.; Diyabalanage, H. V. K.; Rasika Dias, H. V. *Inorg. Chem.* **2003**, *42*, 8612.

Conclusions

In this work, we have synthesized a series of Ag/1,2,4-triazole/polyoxometalate hybrid compounds, which present novel supramolecular assemblies between low-dimensional Ag−1,2,4-triazolate units and POMs. The reflectance spectrum measurements reveal that these inorganic−organic hybrid compounds are potential semiconductor materials. Moreover, these compounds also exhibit interesting photoluminescence phenomena, including O → Mo [LMCT] and intraligand [$\pi-\pi^*$] emissions generated by an internal heavy metal effect. In all, it is reasonable to believe that the present work is important to expand the application of POM-based materials.

Acknowledgment. This work was supported by the 973 key program of the MOST (2006CB932904), the National Natural Science Foundation of China (20425313, 20521101, 20333070, and 90206040), the Chinese Academy of Sciences (KJCX2-YW-M05), and the Natural Science Foundation of Fujian Province (2005HZ01-1).

Supporting Information Available: X-ray crystallographic files in CIF format and additional plots of the structures, FT-IR spectra, ESR spectra, diffuse reflectance (DR) results, and thermogravimetric analysis for the complexes in PDF format. This material is available free of charge via the Internet at http://pubs.acs.org. CCDC-613927 (**1**), 604131 (**2**), 604132 (**3**), 604133 (**4**), 613928 (**5**), 613931 (**6**), 613930 (**7**), and 613929 (**8**) contain the supplementary crystallographic data for this paper. These data can be obtained free of charge from The Cambridge Crystallographic Data Center via www.ccdc.cam.ac.uk/data_ request/cif.

IC700415W

(46) Wang, R. Z.; Xu, J. Q.; Yang, G. Y.; Bu, W. M.; Xing, Y. H.; Li, D. M.; Liu, S. Q.; Ye, L.; Fan, Y. G. *Polyhedron* **1999**, *18*, 2971.